

Response and amplification of terahertz electromagnetic waves in intrinsic Josephson junctions of layered high- T_c superconductor

Shi-Zeng Lin and Xiao Hu

WPI Center for Materials Nanoarchitectonics, National Institute for Materials Science, Tsukuba 305-0044, Japan
and Japan Science and Technology Agency, 4-1-8 Honcho, Kawaguchi, Saitama 332-0012, Japan

(Received 28 January 2010; revised manuscript received 17 May 2010; published 12 July 2010)

We investigate the response of a stack of intrinsic Josephson junctions (IJJs) to terahertz (THz) electromagnetic (EM) irradiation. A significant amplification of the EM wave can be achieved by the IJJs stack when the incident frequency equals to one of the cavity frequencies. The irradiation excites π -phase kinks in the junctions, which stimulate the cavity resonance when the bias voltage is tuned. A large amount of dc energy is then pumped into the Josephson plasma oscillation and the incident wave gets amplified. From the profound current step in IV characteristics induced at the cavity resonance, the system can also be used for detection of the THz wave.

DOI: [10.1103/PhysRevB.82.020504](https://doi.org/10.1103/PhysRevB.82.020504)

PACS number(s): 74.50.+r, 85.25.Cp, 74.25.Gz

It has been known for a long time that Josephson junctions can be used as oscillator, amplifier, and detector for electromagnetic (EM) wave.¹ The operating frequency of these devices made of conventional low-temperature superconductors is below terahertz (THz) due to the small superconducting energy gap. The discovery of intrinsic Josephson effect in layered high- T_c superconductors,² such as $\text{Bi}_2\text{Sr}_2\text{CaCu}_2\text{O}_{8+\delta}$ (BSCCO), has extended the frequency to the THz band, where EM waves have potential for wide applications,^{3,4} and thus has stimulated intensive research activities in the field.⁵

A breakthrough in generating coherent THz emission has been achieved recently based on a mesa structure of BSCCO single crystal.⁶ Due to the thickness much smaller than the wavelength of EM wave, the IJJs stack itself forms a cavity, synchronizes the plasma oscillation, and radiates coherent THz wave at the cavity resonance.⁷ The dynamics of the superconductivity phase has been addressed theoretically^{8,9} that $\pm\pi$ -phase kinks are developed in the junctions, which couple the dc bias to the standing wave and make the cavity resonance possible.

In applications, THz detector and amplifier are as important as generator. Shapiro steps¹⁰ were observed in IJJs stacks of small BSCCO mesas under THz irradiation,¹¹⁻¹⁴ which can be used for detection. To the best of our knowledge, no experiment on amplification of THz waves based on IJJs has been reported so far. Now with the success of generation of coherent THz wave at cavity resonance,⁶ it is intriguing to explore the possibility of the same setup for the usage of amplification and detection of THz waves, with the expectation that the system exhibiting a cavity resonance in the THz band responds more sensitively to an incident wave than short junctions reported in literatures.

When a stack of IJJs is irradiated by an EM wave, the transmitted wave excites Josephson plasma oscillations inside the IJJs. The incident wave can be either damped or amplified according to the detailed compensation between dissipations caused by quasiparticles and the power supply from the bias voltage, which, in turn, is governed by the phase dynamics in the stack of IJJs.

By investigating the inductively coupled sine-Gordon

equations under appropriate boundary condition taking into account the THz EM irradiation, we show in the present Rapid Communication that with the IJJs stack, one can achieve a significant amplification of the input wave with frequency equal to the one of the cavity frequencies. Tuning the bias voltage, π -phase kinks are created in the junctions, which pumps a large amount of dc energy into the Josephson plasma oscillation due to the cavity resonance. The profound current step in IV characteristics induced at the cavity resonance signals the existence incident THz wave, and thus can be used for detection.

The setup is shown in Fig. 1, where a stack of IJJs is sandwiched by two ideal conductors with infinite thickness. These two conductors prevent the interference between EM waves from the two edges of IJJs stack. The left side of IJJs is exposed to irradiation. We assume that the IJJs are infinitely long in the y direction, and thus the problem reduces to two dimensions with sizes L_x and L_z . This setup is similar to the one proposed in Ref. 15, except for the lateral size $L_x \approx 100 \mu\text{m}$ which contains cavity modes in the THz regime.

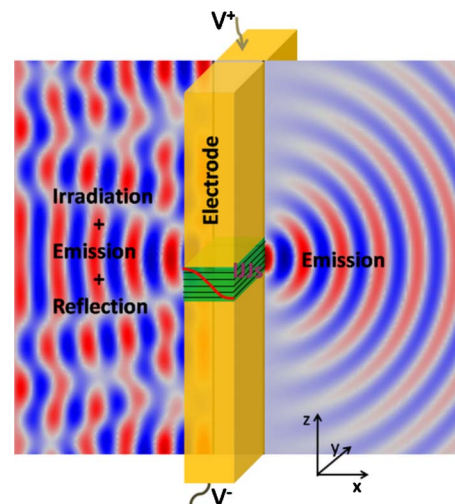


FIG. 1. (Color online) A stack of IJJs sandwiched by two electrodes and subjected to irradiation. The whole setup is immersed in a dielectric material with dielectric constant ϵ_d .

The dynamics of the gauge-invariant phase difference in IJJs is described by the inductively coupled sine-Gordon equations,^{5,8,16,17}

$$\partial_x^2 P_l = (1 - \zeta \Delta_d) [\sin P_l + \beta \partial_t P_l + \partial_t^2 P_l - J_{\text{ext}}], \quad (1)$$

where P_l is the gauge-invariant phase difference at the l th junction, $\beta \equiv 4\pi\sigma_c\lambda_c/c\sqrt{\epsilon_c}$ the normalized c -axis conductivity, $\zeta = (\lambda_{ab}/s)^2$ the inductive coupling; ϵ_c is the dielectric constant and σ_c is the conductivity along the c axis, and s is the lattice period in the c direction; c is the light velocity in vacuum; λ_c and λ_{ab} are the penetration depths along the ab axis and c axis, respectively. In Eq. (1), the lateral space is normalized by λ_c , time by the Josephson plasma frequency $\omega_J = c/\lambda_c\sqrt{\epsilon_c}$, and the external current J_{ext} by the Josephson critical current J_c .¹⁸ Δ_d is the second-order difference operator defined as $\Delta_d f_l \equiv f_{l+1} + f_{l-1} - 2f_l$. We adopt $\beta = 0.02$ and $\zeta = 7.1 \times 10^4$, which are typical for BSCCO.¹⁹ The physics discussed below is valid in a stack of IJJs with huge ζ , which has not yet been achieved in artificial Josephson-junction stacks.^{16,20}

In the absence of irradiation, the so-called dynamic boundary condition (DBC) was derived based on the Maxwell equations.^{7,21} It is easy to generalize the DBC to incorporate irradiation because Maxwell equations are linear. Assuming the incident wave is a plane wave with the electric field polarized along the z axis and the propagation direction normal to the left edge of IJJs, the total electric field on the left side is

$$E_z(x, z, t) = E_z^i(\omega) \exp[i(-\sqrt{\epsilon_d}\omega x + \omega t + \theta)] + \int dk_x E_z^o(\omega, k_x, k_z) \exp[i(-k_x x + k_z z + \omega t)], \quad (2)$$

where $k_x^2 + k_z^2 = \omega^2$ with E_z^o the outgoing wave comprising the emitted and reflected waves, E_z^i the incident wave with a relative phase difference θ to the Josephson plasma oscillation inside IJJs, ω the frequency, and ϵ_d the normalized dielectric constant of the dielectric medium coupled to the IJJs.¹⁸ For simplicity of analysis, we concentrate in Eq. (2) on the case that the frequency of Josephson plasma determined by the bias voltage according to the ac Josephson relation is equal to the incident frequency since otherwise the response of IJJs is very small.

The EM wave at the right edge comes only from emission. The generalized boundary conditions for the oscillating electromagnetic fields in the real space and frequency domain are given by¹⁵

$$B_y(x=0, \omega) = \frac{E_z(0, \omega)}{Z(\omega)} - 2\sqrt{\epsilon_d} E_z^i(0, \omega) \exp(i\theta), \quad (3)$$

$$B_y(x=L_x, \omega) = -\frac{E_z(L_x, \omega)}{Z(\omega)}, \quad (4)$$

where B_y and E_z are the total oscillating magnetic and electric fields, and $Z(\omega) = 2/\{k_\omega L_x \sqrt{\epsilon_d} [1 + \frac{2i}{\pi} \ln \frac{5.03}{k_\omega L_x}]\}$ with $k_\omega \equiv \omega\sqrt{\epsilon_d}$ is the impedance.⁷ The power of the incident wave is $S_i = \sqrt{\epsilon_d} (E_z^i)^2/2$. Since the thickness of the IJJs stack used in

experiments is $L_z = 1 \mu\text{m}$, much smaller than the wavelength in the THz band, the electromagnetic fields are uniform in the z direction in the IJJs for THz waves as in Eqs. (3) and (4). There exists a significant impedance mismatch between the IJJs and the dielectric medium, which is crucial for the cavity resonances. With the relations $(1 - \zeta \Delta_d) B_l^y = \partial_x P_l$ and $E_l^z = \partial_t P_l$,¹⁹ one obtains the boundary condition for the oscillating part of P_l .

A solution to Eq. (1) is given intuitively by

$$P_l(x, t) = \omega t + \text{Re}[-ig(x)\exp(i\omega t)], \quad (5)$$

where the first term at the right-hand side is the uniform rotating phase according to the ac Josephson relation and the second term is the plasma oscillation. The spatial modulation of plasma oscillation is induced by both radiation and irradiation. We consider the region of small plasma oscillation $|g(x)| < 1$. From terms with time dependence $\exp(\pm i\omega t)$, we obtain the equation for $g(x)$ by substituting Eq. (5) into Eq. (1),

$$\partial_x^2 g(x) = 1 + i\beta\omega g(x) - g(x)\omega^2. \quad (6)$$

Equation (6) has the solution

$$g(x) = A + a \exp(iqx) + b \exp(-iqx) \quad (7)$$

with $A = 1/(\omega^2 - i\beta\omega)$ and $q \approx \omega$ for weak damping $\beta \ll 1$ as in the case of BSCCO system. The first term A in Eq. (7) represents the uniform plasma oscillation and the other two terms are propagating waves due to radiation and irradiation, with the two coefficients a and b determined by the boundary condition in Eqs. (3) and (4).

The IV characteristics is derived from the current conservation relation

$$J_{\text{ext}} = \beta\omega + \langle \sin P_l \rangle_{xt}, \quad (8)$$

where $\langle \dots \rangle_{xt}$ denotes the average over space and time. Besides the normal current due to the quasiparticles $J_n = \beta\omega$, the total dc current has two contributions from the plasma oscillation due to the nonlinearity of the dc Josephson effect: $J_p = \beta/[2(\omega^3 + \beta^2\omega)]$ and $J_w = \{a[1 - \exp(i\omega L_x)] - b[1 - \exp(-i\omega L_x)]\}/(2\omega L_x)$ associated with the uniform and nonuniform parts of plasma oscillation in Eq. (7). The IV curves for different θ 's are displayed in Fig. 2(a) for the incident wave $S_i = 141 \text{ W/cm}^2$. When one fixes the voltage satisfying the phase-locking relation and sweeps the current, the relative phase θ adjusts itself to match the current, which traces out the Shapiro steps.¹⁰ Zero-crossing Shapiro steps²² occur at small voltages. For $1/Z \ll \omega L_x \ll 1$, J_w is given explicitly as

$$J_w = \text{Re} \left[\frac{1}{L_x \omega^3 Z} - \frac{E_z^i e^{i\theta} \sqrt{\epsilon_d}}{L_x \omega^2} \right]. \quad (9)$$

J_w is maximized (minimized) at $\theta = \pi$ ($\theta = 0$) and the height of the Shapiro step is given by $J_s = 2E_z^i \sqrt{\epsilon_d}/L_x \omega^2$. In the region where $\Delta J_w \equiv J_w(E_z^i > 0) - J_w(E_z^i = 0) > 0$, a dc power $\Delta J_w \omega$ is converted into emission. When $J_w < 0$, the incident EM wave is converted into dc power and charges the IJJs, and the IJJs effectively work as a battery.

The radiation powers measured by the Poynting vector

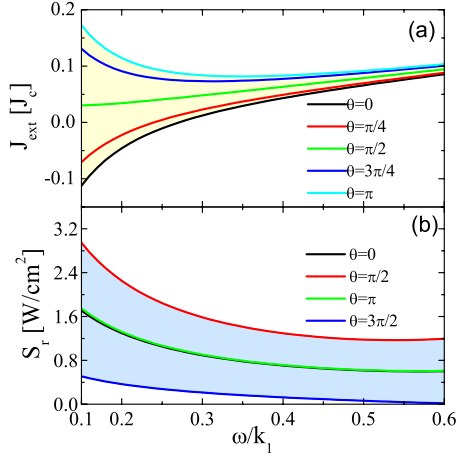


FIG. 2. (Color online) (a) IV characteristics and (b) radiation power at the right edge of the state described by Eq. (5) for the incident wave of $S_i=141$ W/cm² at several typical phases θ . The light yellow (shaded) region in between the maximal and minimal current associated with $\theta=0$ and $\theta=\pi$ is the width of the first Shapiro step. The results are obtained with $L_x=80$ μm , $L_z=1$ μm , and $\epsilon_d=0.1$ similar to those in the experiments (Ref. 6).

satisfy the power balance condition $S_r - S_l + P_d = J_{\text{ext}}\omega$ with P_d the dissipation caused by the quasiparticles, and S_l and S_r the radiation at the left and right edge, respectively. The emission at the right edge is depicted in Fig. 2(b) for $S_i=141$ W/cm². It is clear that the emission is always very weak because of lack of an efficient way to pump energy into the plasma oscillation in this state. In the same limit, the radiation power is given by

$$S_r = \text{Re} \left[\frac{\omega^2}{2Z^*} \right] \left| A - \frac{2iE_z^i e^{i\theta} \sqrt{\epsilon_d}}{L_x \omega^2} \right|^2. \quad (10)$$

It is clear that the emission comprises of spontaneous one $S_{\text{sp}} \sim |A|^2$, the one caused by transmitted wave $S_{\text{tw}} \sim |E_z^i|^2$ and the stimulated one $S_{\text{st}} \sim |E_z^i A|$.

The state given in Eq. (5) is found to become unstable when the incident frequency and the bias voltage get close to $\omega=k_1 \equiv \pi/L_x$, where the cavity mode $g(x) \approx A_1 \cos(k_1 x)$ with $A_1 > 1$ is induced by the irradiation (without losing generality, here we consider the first cavity mode). Instead of Eq. (5) the phase dynamics should then be described by⁸

$$P_l(x, t) = \omega t + P_l^s(x) + \text{Re}[-ig(x)\exp(i\omega t)], \quad (11)$$

where P_l^s is the static phase kink associated with the cavity mode. Substituting Eq. (11) into Eq. (1), we obtain the following equations:

$$\partial_x^2 g(x) = (1 - \zeta \Delta_d) \exp(iP_l^s) + i\beta\omega g(x) - g(x)\omega^2 \quad (12)$$

and

$$\partial_x^2 P_l^s = \frac{i}{2} \zeta \Delta_d g(x) \exp(-iP_l^s). \quad (13)$$

Since the Josephson plasma should take the form

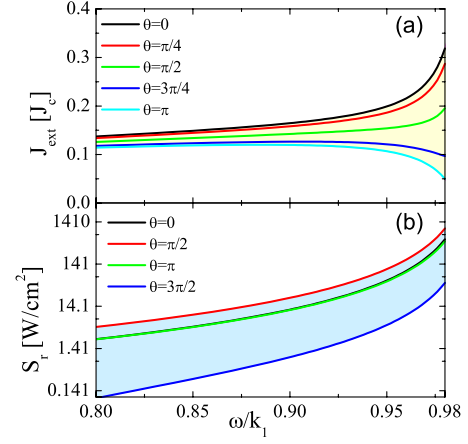


FIG. 3. (Color online) (a) IV characteristics and (b) radiation power when the π -phase kinks are excited near the cavity resonance. Other parameters are the same as those in Fig. 2.

$$g(x) = A_1 \cos k_1 x + a \exp(iqx) + b \exp(-iqx), \quad (14)$$

where $q \approx \omega$, we arrive at $A_1 = F_1 / (ik_1^2 - i\omega^2 - \beta\omega)$ with $F_1 = \frac{-2i}{L_x} \int_0^{L_x} (1 - \zeta \Delta_d) \exp(iP_l^s) \cos(k_1 x) dx$. Due to that the dominant term in Eq. (14), $g(x) \approx A_1 \cos(k_1 x)$ is antisymmetric with respect to $x=L_x/2$, Eq. (13) has a solution of π kinks alternatingly piled up in the c axis.⁸ Because of the huge inductive coupling $\zeta \approx 10^5$ in BSCCO, the phase kinks render themselves as step functions, and are stable against the radiation and irradiation provided $|a|, |b| < |A_1|$. The width of a kink should be smaller than the junction width $1/\sqrt{|A_1|} \zeta < L_x$, which gives an estimate on the regime where the kink state is stable.

Although it has been revealed theoretically that the π -kink state is ideal for generating strong terahertz electromagnetic waves,^{5,8} the dynamic process to realize the state was not clear. The present study indicates that irradiating the junction stack by an incident wave can stimulate the π -kink state.

The dc supercurrent induced by the plasma oscillation in the kink state can be evaluated by $\langle -ig(x)\exp(-iP_l^s)/2 \rangle_x$. It includes the current associated with the plasma oscillations at the cavity mode $J_p = 4\beta\omega / \{\pi^2[(k_1^2 - \omega^2)^2 + \beta^2\omega^2]\}$, and that with radiation and irradiation $J_w = (a[\exp(i\omega L_x/2) - 1]^2 - b[\exp(-i\omega L_x/2) - 1]^2) / (2\omega L_x)$. The IV characteristics with the irradiation of $S_i=141$ W/cm² are given in Fig. 3(a). For $1/Z \ll k_1 - \omega \ll 1$ and $(k_1^2 - \omega^2) \gg \beta\omega$, we have

$$J_w = \text{Re} \left[\frac{8}{L_x \pi^2 Z (k_1^2 - \omega^2) (k_1 - \omega)} + \frac{2E_z^i e^{i\theta} \sqrt{\epsilon_d}}{\pi^2 (k_1 - \omega)} \right]. \quad (15)$$

Because of the π -phase kinks, now J_w is maximized (minimized) at $\theta=0$ ($\theta=\pi$) in contrast to Eq. (9). The height of the Shapiro step is $J_s = 4E_z^i \sqrt{\epsilon_d} / [\pi^2(k_1 - \omega)]$. As is well known, Shapiro steps are suppressed by internal modes in single junctions. It is the same case for a IJJs stack if the state is uniform along the c axis since Eq. (1) is decoupled. Therefore, the appearance of a Shapiro step at the cavity resonance can be used as an exclusive detection of the π -kink state in a stack of IJJs.

The radiation power at the right edge is depicted in Fig. 3(b) for $S_i=141$ W/cm². It is clear that the input wave is enhanced significantly near the cavity frequency, where the π kinks stimulated by the irradiation pump a large amount of dc power from the dc bias into Josephson plasma oscillation.

The radiation power at the right edge in the same limit is given by

$$S_r = \text{Re} \left[\frac{\omega^2}{2Z^*} \right] \left| -\frac{4}{\pi(k_1^2 - \omega^2)} + \frac{2iE_z^i e^{i\theta} \sqrt{\epsilon_d}}{\pi(k_1 - \omega)} \right|^2. \quad (16)$$

An amplification factor can be defined by the maximal value of the ratio S_r/S_i with respect to the phase θ for a given S_i . For the π -kink state, one has

$$f_a = \text{Re} \left[\frac{\omega^2}{\sqrt{\epsilon_d} Z^*} \right] \left| \frac{4}{\pi(k_1^2 - \omega^2) E_z^i} + \frac{2\sqrt{\epsilon_d}}{\pi(k_1 - \omega)} \right|^2, \quad (17)$$

which is achieved at $\theta=\pi/2$. As displayed in Fig. 4, the amplification factor reaches its maximum at $\omega=k_1$. An incident wave of power of 141 W/cm² can be amplified by one order of magnitude. The amplification factor decreases with the power of incident wave, and the maximum power which can be amplified by this technique is estimated as 3000 W/cm².

In a single junction, the presence of irradiation may cause chaotic dynamics in a certain parameter space,²² which is harmful for applications. The chaos can be avoided when the frequency of the incident wave is much larger than the Josephson plasma frequency,^{12,22} which is fulfilled in a IJJs stack of length smaller than λ_c .

In conclusion, simultaneously shining a terahertz electromagnetic wave and biasing a dc voltage on a stack of intrinsic

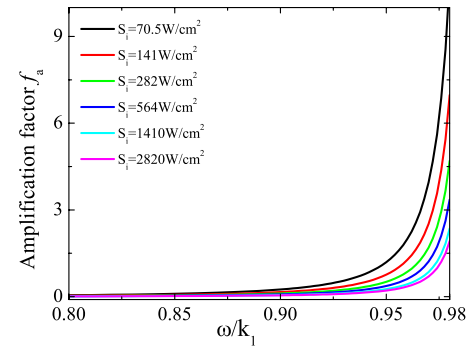


FIG. 4. (Color online) Amplification factor for several typical incident powers near the cavity resonance.

Josephson junctions stimulates the standing wave of Josephson plasma, which develops π -phase kinks in the junctions, when the frequency equals to one of the cavity frequencies of the junction stack. At the cavity resonance, the rotating π kinks pump a large amount of dc energy into Josephson plasma oscillation, and the incident wave gets amplified. The maximal radiation power reached by this terahertz amplifier is estimated as 3000 W/cm². Since the strong plasma oscillation induces a large dc supercurrent at the cavity resonance, the system can work as a terahertz detector. The response of the system to irradiation depends on the spatial structure of the superconductivity phase, thus the phase dynamics may be probed by the irradiation.

This work was supported by WPI Initiative on Materials Nanoarchitectonics, MEXT, Japan and CREST-JST Japan. Calculations were performed on the Numerical Materials Simulator (SGI Altix supercomputer) in NIMS.

¹A. Barone and G. Paterno, *Physics and Applications of the Josephson Effect* (Wiley, New York, 1982).

²R. Kleiner, F. Steinmeyer, G. Kunkel, and P. Müller, *Phys. Rev. Lett.* **68**, 2394 (1992).

³B. Ferguson and X. C. Zhang, *Nature Mater.* **1**, 26 (2002).

⁴M. Tonouchi, *Nat. Photonics* **1**, 97 (2007).

⁵X. Hu and S. Z. Lin, *Supercond. Sci. Technol.* **23**, 053001 (2010).

⁶L. Ozyuzer, A. E. Koshelev, C. Kurter, N. Gopalsami, Q. Li, M. Tachiki, K. Kadowaki, T. Yamamoto, H. Minami, H. Yamaguchi, T. Tachiki, K. E. Gray, W.-K. Kwok, and U. Welp, *Science* **318**, 1291 (2007).

⁷L. N. Bulaevskii and A. E. Koshelev, *Phys. Rev. Lett.* **97**, 267001 (2006).

⁸S. Z. Lin and X. Hu, *Phys. Rev. Lett.* **100**, 247006 (2008).

⁹A. E. Koshelev, *Phys. Rev. B* **78**, 174509 (2008).

¹⁰S. Shapiro, *Phys. Rev. Lett.* **11**, 80 (1963).

¹¹Y. J. Doh, J. H. Kim, K. T. Kim, and H. J. Lee, *Phys. Rev. B* **61**, R3834 (2000).

¹²H. B. Wang, P. H. Wu, and T. Yamashita, *Phys. Rev. Lett.* **87**,

107002 (2001).

¹³Y. I. Latyshev, M. B. Gaifullin, T. Yamashita, M. Machida, and Y. Matsuda, *Phys. Rev. Lett.* **87**, 247007 (2001).

¹⁴M. H. Bae, R. C. Dinsmore, M. Sahu, H. J. Lee, and A. Bezryadin, *Phys. Rev. B* **77**, 144501 (2008).

¹⁵L. N. Bulaevskii, A. E. Koshelev, and M. Tachiki, *Phys. Rev. B* **78**, 224519 (2008).

¹⁶S. Sakai, P. Bodin, and N. F. Pedersen, *J. Appl. Phys.* **73**, 2411 (1993).

¹⁷L. N. Bulaevskii, D. Domínguez, M. P. Maley, A. R. Bishop, and B. I. Ivlev, *Phys. Rev. B* **53**, 14601 (1996).

¹⁸S. Z. Lin, X. Hu, and M. Tachiki, *Phys. Rev. B* **77**, 014507 (2008).

¹⁹S. Z. Lin and X. Hu, *Phys. Rev. B* **79**, 104507 (2009).

²⁰A. V. Ustinov, H. Kohlstedt, M. Cirillo, N. F. Pedersen, G. Hallmanns, and C. Heiden, *Phys. Rev. B* **48**, 10614 (1993).

²¹A. E. Koshelev and L. N. Bulaevskii, *Phys. Rev. B* **77**, 014530 (2008).

²²R. L. Kautz, *Rep. Prog. Phys.* **59**, 935 (1996).